Received: 4 August 2023 | Accepted: 15 August 2023

DOI: 10.1111/eos.12951

European Journal of Oral Sciences | NOF Scandinavian Division IADR | WILEY

ORIGINAL ARTICLE

Load-bearing capacity and wear characteristics of short fiber-reinforced composite and glass ceramic fixed partial dentures

Enas Mangoush[1] | **Sufyan Garoushi**[1] | **Pekka Vallittu**[1,2] | **Lippo Lassila**[1]

[1]Department of Biomaterials Science and Turku Clinical Biomaterial Center -TCBC, Institute of Dentistry, University of Turku, Turku, Finland

[2]Wellbeing Services County of South-West Finland, Turku, Finland

Correspondence
Enas Mangoush, Institute of Dentistry and TCBC, University of Turku, Itäinen Pitkäkatu 4 B Turku, 20520, Finland.
Email: enas.mangoush@utu.fi

The aim of this study was to evaluate load-bearing capacity and wear performance of experimental short fiber-reinforced composite (SFRC) and conventional lithium-disilicate CAD/CAM fabricated fixed partial dentures (FPDs). Two groups (n = 12/group) of three-unit CAD/CAM fabricated posterior FPDs were made. The first group used experimental SFRC blocks, and the second group fabricated from lithium-disilicate (IPS e.max CAD). All FPDs were luted on a zirconia testing jig with dual-curing resin cement. Half of FPDs per group were quasi-statically loaded until fracture. The other half experienced cyclic fatigue aging (100.000 cycles, Fmax = 500 N) before loading quasi-statically until fracture. Fracture mode was examined using SEM. Wear test was performed using 15,000 loading cycles. Both material type and aging had a significant effect on the load-bearing capacity of FPDs. Experimental SFRC CAD without fatigue aging had significantly the highest load-bearing capacity (2096 ± 149N). Cyclic fatigue aging decreased the load-bearing capacity of the SFRC group (1709 ± 188N) but increased it for the lithium-disilicate group (1546 ± 155N). Wear depth values of SFRC CAD (29.3μm) were significantly lower compared to lithium-disilicate (54.2μm). Experimental SFRC CAD demonstrated the highest load-bearing capacity before and after cyclic fatigue aging, and superior wear behavior compared to the control material.

KEYWORDS
abrasive wear, CAD/CAM restoration, fatigue aging, fracture load, teeth supported fixed prosthesis

INTRODUCTION

Three-unit fixed partial dentures (FPDs) are a practicable prosthetic intervention for compensating a missing tooth and can be employed as an alternative to single-implant restorations when appropriate indications are met [1].

A variety of materials are available for the production of three-unit FPDs based on the intended duration and indication such as restoration length. During the last few decades, FPDs were commonly made with metal frameworks veneered with ceramic. Despite their favorable mechanical properties and longevity, metal-based FPDs were frequently linked to aesthetic drawbacks. Consequently, metal-free veneered and monolithic all-ceramic systems have grown in popularity to fabricate FPDs [2].

For anterior teeth, all-ceramic FPDs have similar clinical results to metal-ceramic restorations; however, for posterior teeth, all-ceramic FPDs, particularly those with veneered

frameworks, are more likely to experience chipping, cracking, or delamination [3, 4]. These issues arise from several contributing factors, including the veneering porcelain's low fracture toughness and strength [5], thermal incompatibility among the materials, and low bond strength between the veneering porcelain and infrastructure materials [4, 6, 7].

To address these problems, all-ceramic systems that have better mechanical and thermal properties have been developed. For example, zirconia and lithium-disilicate bridges are fabricated using computer-aided design/computer-aided manufacturing (CAD/CAM) technology, which can ensure a precise fit and optimal functionality. Both materials provide excellent mechanical strength, superior fracture resistance, and offer aesthetic advantages resulting in natural-looking posterior restorations [8]. However, some limitations and drawbacks are also recorded for all-ceramic systems. All-ceramic restorations tend to be more expensive than other alternatives, such as metal or metal-ceramic restorations, and they can potentially cause more wear on opposing natural teeth in addition to their limited repair options [9]. Moreover, it is important to note that some popular monolithic all-ceramic materials, for example, IPS e.max, are indicated for restorations of three-unit bridges only up to the second premolar as the terminal abutment, and therefore they are not recommended when molars need to be restored [10].

Regarding zirconia, in vitro studies and systematic reviews have come to the conclusion that establishing a strong and durable bond between zirconia and the cementing agent can raise challenges in ensuring long-term durability [11, 12].

CAD/CAM polymers and polymethyl methacrylate-based composites have been previously used to address the requirements for temporary FPDs. However, when they started to be employed as posterior permanent restorations, the usage of CAD/CAM composite has been restricted to single-tooth restorations. In the literature, an assessment of the material's susceptibility to catastrophic fracture has indicated that a low elastic modulus of the FPD framework material, combined with high resiliency, can result in a more homogeneous distribution of stress within the framework [13]. Moreover, in comparison to ceramics, CAD/CAM composites are known for their superior damage tolerance and reduced brittleness, which results in the formation of smoother margins and reduced marginal chipping [14]. These significant properties have guided attempts to use the CAD/CAM composite restoration as a suitable alternative for the indication of multi-unit permanent FPDs.

Short fiber-reinforced composites (SFRCs) with their enhanced mechanical characteristics have been mainly introduced to reinforce composite restorations in high stress-bearing areas as a direct bulk-fill or flowable restorative material [15–17]. SFRC showed the high performance necessary to augment load-bearing capacity and alter the fracture pattern to more repairable forms [18–21].

TABLE 1 CAD/CAM materials used with their composition.[a]

Material	Manufacturer	Composition (wt%)
IPS e.max CAD	Ivoclar Vivadent ,	Silicon dioxide 57%–80%, lithium oxide 11%–19%, potassium oxide 0%–13%, phosphorus oxide 0%–11%, and other oxides
SFRC CAD	Experimental	UDMA, TEGDMA, short glass fiber (200–300 μm & Ø7 μm), barium glass 77 wt%

Abbreviations: CAD/CAM, computer-aided design/computer-aided manufacturing; TEGDMA, triethylene glycol dimethacrylate; UDMA, urethane dimethacrylate; wt%, weight percentage.

[a]Composition based on manufacturer details.

In posterior teeth, where we have high stress-bearing areas, the material's capacity to withstand wear is also a crucial factor to consider, since it is one of the responsible factors for the long-term quality of the restoration under occlusal forces. Over the years, the wear characteristics of composites have been enhanced; however, despite these improvements, composites are still not considered to have ideal resistance to wear. The suboptimal wear resistance is seen as one of the primary limitations of the composites [22]. The wear characteristics of direct SFRC have been investigated in previous studies, and it has been found that the incorporation of short fibers into the composite does not have a negative impact on its wear [23, 24].

Experimental indirect SFRC CAD composites have been tested to investigate their mechanical, optical, surface, and bonding properties [21, 23, 25]. Moreover, their fracture behavior when used as inlay-retained FPDs has resulted in encouraging outcomes [26]. However, up to now, there are no available data on the load-bearing capacity of SFRC CAD when used as conventional three-unit FPDs in the posterior region.

It is noteworthy that studies comprehensively combining both load-bearing capacity and wear characteristics remain remarkably limited in the literature. Therefore, in this study, we aimed to bridge this gap by evaluating the load-bearing capacity of FPDs before and after cyclic fatigue aging and the wear properties of the tested materials simultaneously. The suggested hypothesis was that both the material type and aging procedure would have no impact on the fracture behavior and wear characteristics of the FPDs.

MATERIAL AND METHODS

The materials used in this study are listed in Table 1.

European Journal of Oral Sciences

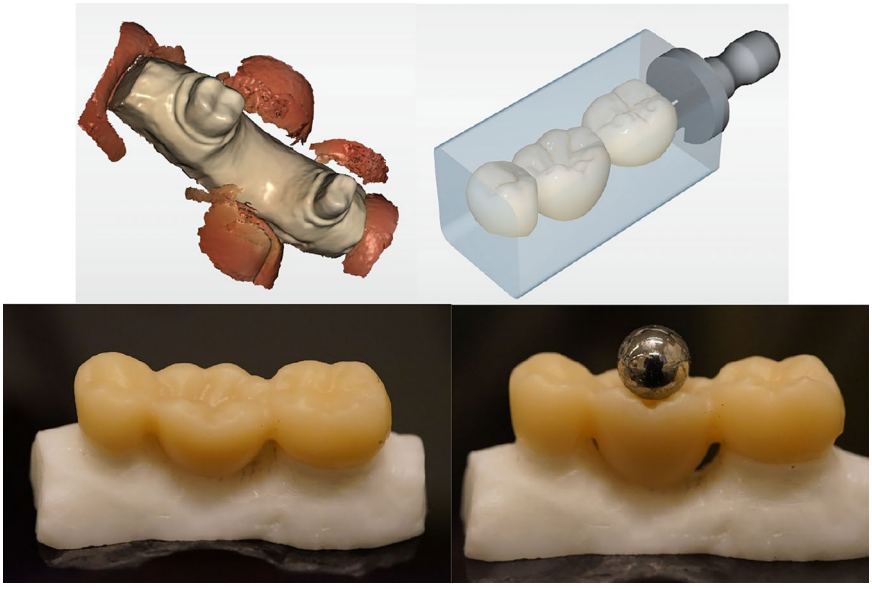

FIGURE 1 Pictures showing the zirconia model, the specimen before and after milling process, and loading test setup. Loading was applied vertically between the triangular ridges of the lingual and buccal cusps.

Fabrication of FPD specimens

To create the FPD restoration model, a zirconia model was cut from a pre-sintered zirconium oxide blank (Zirconia Prettau VR 95H22; Zirkonzahn) using a CAD/CAM device (5-TEC; Zirkonzahn). The framework design resembled a three-unit full-coverage FPD from the second premolar to the second molar to replace the missing first molar (Figure 1). The abutments were made with 1.5-mm axial shoulder reductions in accordance with the cemento-enamel junction. The axial reduction was measured from the preparation margins, and then a 2 mm occlusal reduction was conducted, keeping, a 10 mm distance between the two abutments, as it simulated the crown dimension of the mandibular first molar. A digital impression of the zirconia model was acquired using another dental CAD/CAM device (CEREC Omnicam AC; Dentsply Sirona). Consequently, a three-unit FPD was designed, encompassing the area from the second premolar to the second molar to replace the missing first molar, measuring 9.5 mm in buccolingual width and 10 mm in mesiodistal width (Figure 1).

A total of 24 FPDs were allocated to two groups (lithium-disilicate and SFRC; n = 12/group) according to their fabrication materials. FPDs made of lithium-disilicate CAD blocks underwent the crystallization process in a ceramic oven (Programat P310; Ivoclar Vivadent) following the manufacturer's guidelines. Finishing and polishing procedures for all FPDs were carried out in accordance with the manufacturer's provided instructions.

Prior to luting, the internal surface of all FPDs was acid etched (<5%) using hydrofluoric acid (IPS Ceramic etching gel; Ivoclar Vivadent) for 20 s, followed by rinsing, air-drying, and the application of primer (G-Multi Primer; GC).

The FPDs were then cemented to the abutment with dual-cure resin cement (G-Cem One; GC). A hand-light curing unit (Elipar TM S10, 3 M ESPE) was then employed for light curing from all directions, with each segment receiving 20 s of exposure (the light wavelength ranged from 430 to 480 nm, and the light intensity was 1600 mW/cm^2). The light source was positioned in close proximity to the crown surface.

Fracture load test

Half of the FPDs per group (n = 6) were exposed to cyclic fatigue aging before undergoing a static fracture load test. The zirconia model was positioned securely in a water bath (room temperature) and placed in a universal testing machine Z010 (Zwick/Roell). The FPDs underwent a series of dynamic mechanical loading cycles, totaling 100,000 cycles, where a maximum force of 500 N was applied for 20 s at a frequency of 1.2 Hz. Specimens were immersed under water during cyclic aging for one week. The other half of the FPDs in each group (n = 6/group) were subjected directly to a quasi-static load. This load was directly applied using a universal testing machine (Lloyd model LRX; Lloyd Instruments) at 1 mm/min speed. The loading was vertically applied between the triangular ridges of the buccal and lingual cusps, as shown in Figure 1, using a metal ball with a diameter of 5 mm. The loading event was recorded until the restoration fractured, indicated by a significant drop in the load-deflection curve (Figure 4).

Two-body wear test

Block-shaped specimens of each material, measuring 14 mm in length, 12 mm in width, and 2 mm in thickness, were immersed in water at 37°C for one day. A two-body wear

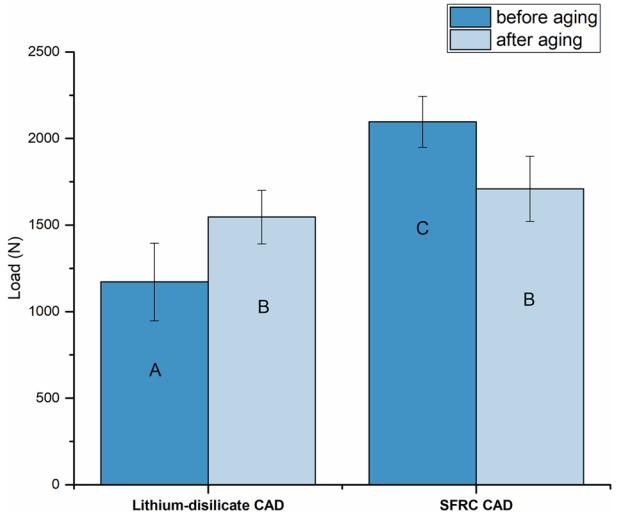

FIGURE 2 Standard deviation and mean values of load-bearing capacity (*N*) of tested fixed partial dentures both before and after cyclic fatigue aging. Different letters indicate statistically significant differences between groups. CAD, computer-aided design; SFRC, short fiber-reinforced composite.

test was conducted using a chewing simulator (CS-4.2; SD Mechatronik) equipped with two chambers to simulate horizontal and vertical movements simultaneously, all submerged in water. In each chamber, an upper specimen holder secured the loading tip with a screw, and a lower specimen holder made of plastic housed the embedded specimen to be used as antagonistic wear material. The upper specimen holders contained manufacturer-standard loading balls (Steatite ball, Ø 6 mm) embedded in acrylic resin, securely fastened with a screw. For each experiment, a new ball was used.

The wear test involved a 2 kg weight, equivalent to a chewing force of 20 N, with 15,000 loading cycles at a frequency of 1.5 Hz. After each test, the wear patterns on the surface of each specimen ($n = 6$) were analyzed using a three-dimensional non-contact optical profilometer (Bruker Nano) with Vision64 software (Bruker Nano). From various points on the surface, the maximum wear depth values (μm) were measured, representing the average of the deepest points obtained from all profile scans.

Microscopic analysis

All FPD specimens were first cleaned properly in an ultrasonic bath, then dried and subsequently coated with a gold layer using a sputter coater in a vacuum evaporator (BAL-TEC SCD 050 Sputter Coater) to prepare them for observation. Images of scanning electron microscopy (SEM) (LEO) were used to show the effect of loading on the investigated materials under 30, 250, 500, 1000, and 2500× magnification, and materials surfaces after the two-body wear test under 50, 500, and 5000× magnification. Analysis of the steatite ball of the chewing simulator was applied using SEM under 30× and 200× magnification to compare the effect of tested materials on the ball surface, which resembles enamel.

Statistical analysis

Statistical analysis of the data was performed using a two-way analysis of variance (ANOVA) followed by the Tukey HSD test ($\alpha = 0.05$) to assess the differences between the load-bearing capacity of tested FPDs using SPSS version 27 (SPSS, IBM Corp). Load-bearing capacity was the dependent variable, and material type and aging procedure were the independent variables. One-way ANOVA was used for wear and Levene's test of equality and error variances was used to test for normal variation in outcomes.

RESULTS

The mean values of fracture load with the standard deviation of the tested FPDs before and after fatigue aging are presented in Figure 2. Levene's test revealed that the error variance of the dependent variable was equal across groups where the load-bearing capacity was the dependent variable. ANOVA demonstrated that material type and aging had a significant effect ($p < 0.05$) on the fracture load values of the FPDs. The experimental SFRC CAD specimens resulted in the highest load-bearing capacity before aging (2096 ± 149 N) ($p < 0.05$), while the lithium-disilicate group showed the lowest value (1170 ± 226 N) ($p < 0.05$). In a direct comparison of each material before and after cyclic fatigue aging, ANOVA results revealed that after applying cyclic fatigue aging, there was a decrease ($p < 0.05$) in the fracture load value of FPDs made of the experimental SFRC CAD (1709 ± 188 N) as shown in Figure 2. However, the fracture load results of FPDs made of lithium-disilicate CAD after aging increased ($p < 0.05$) (1546 ± 155 N) in comparison with the same material without aging.

Upon visual inspection (Figure 3), the specimens exhibited irreparable cracking fracture patterns in the connector region of FPDs of both groups. Despite the presence of numerous cracks, the individual components of the specimens were not detached from one another. Figure 4 displays the load–deflection curves of the specimens before and after fatigue aging, with the SFRC CAD FPDs showing a good capacity to endure loads prior to fracturing.

Figure 5 shows SEM images of the fractured FPDs. Analysis of the experimental SFRC CAD specimens shows how the crack line propagated and how the fibers attenuated the crack in such a way that its width is decreased, and the propagation is hindered by the fiber pullout and bridging

European Journal of Oral Sciences NOF Scandinavian Division IADR WILEY

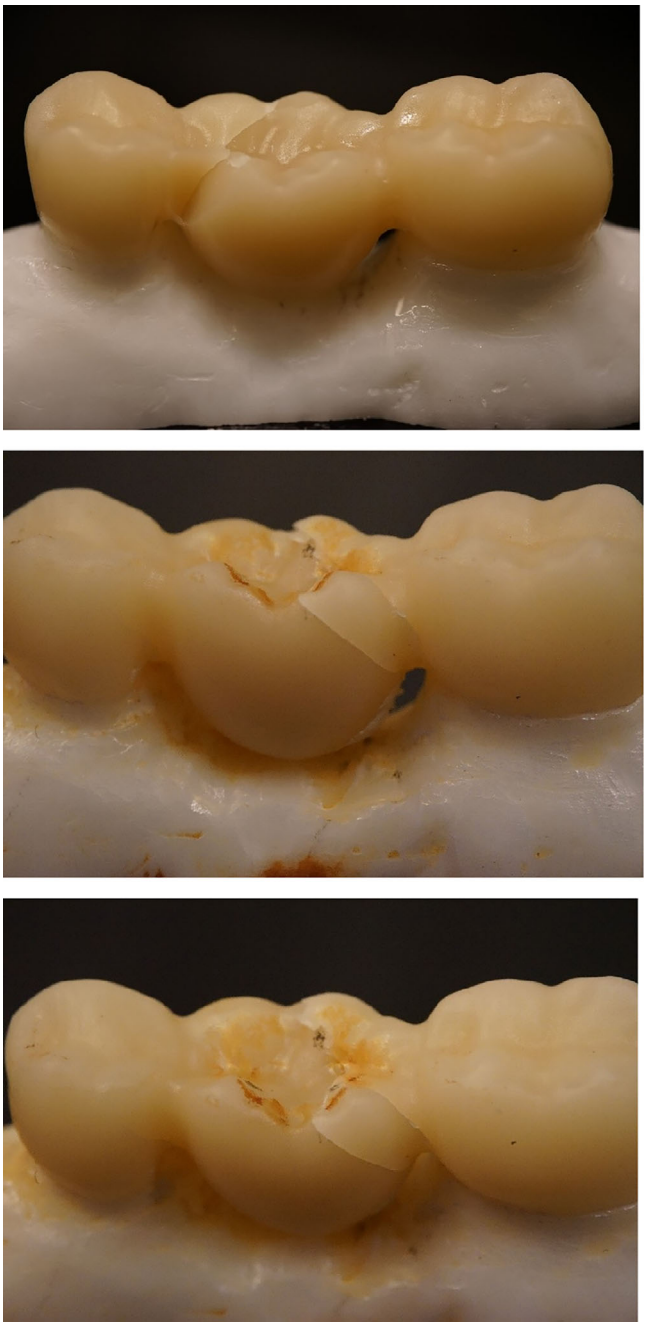

FIGURE 3 Fracture patterns of the tested fixed partial dentures. The top photo shows a fractured specimen subjected to quasi-static loading before aging; the lower photos show the cracking fracture pattern of a specimen subjected to cyclic fatigue aging.

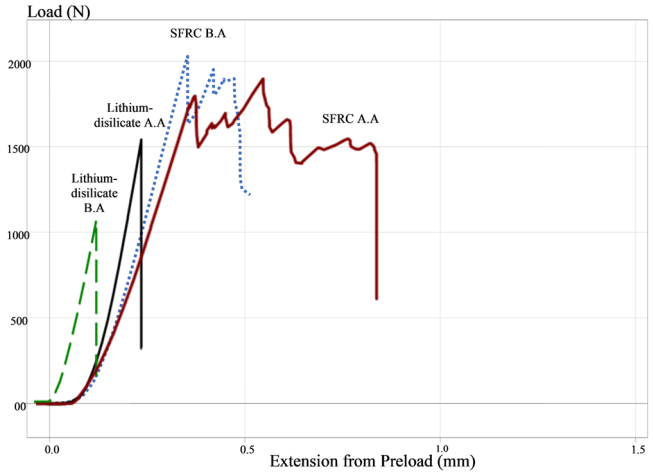

FIGURE 4 Load–deflection curves of typical lithium-disilicate and short fiber-reinforced composite (SFRC) specimens before and after fatigue aging. A.A, after aging; B.A, before aging.

mechanisms. The lithium-disilicate specimens demonstrate the typical characteristics of a radial fracture pattern, which is commonly associated with brittle materials. The cracks tend to be linear, straight, and have sharp edges.

Mean values for wear depth recorded for both materials following 15,000 chewing simulation cycles is shown in Figure 6. The data demonstrate that lithium-disilicate specimens displayed a mean wear depth of 54.2 μm, indicating greater depth compared to the SFRC CAD with a mean wear depth of 29.3 μm ($p < 0.05$).

Representative SEM images of the wear facets for lithium-disilicate and SFRC CAD are shown in Figure 7A,B. The wear facet of lithium-disilicate (Figure 7A1) exhibits a larger size compared to the SFRC CAD facet (Figure 7B1), as evidenced by vertical diameter measurements of 1.556 and 1.116 mm, respectively. This disparity in size occurs even though both facets were subjected to identical loading balls with equivalent weights. The facet surfaces appear to have some variation in texture, with the lithium-disilicate CAD showing smooth scratches running through the length of their wear tracks. Figure 7B2,B3 illustrate that the microfibers of the SFRC CAD had not protruded, but were polished down together with the composite matrix, leaving an almost even, smooth surface.

Analysis of the steatite ball of the chewing simulator (Figure 8A1,A2,B1,B2) shows wider boundaries of wearing facet in the ball used as an antagonist with the lithium-disilicate specimens (1.403 mm for the x-axis, and 1.588 mm for the y-axis; Figure 8A1), while the facet size in the ball used as an antagonist to the SFRC CAD specimen was smaller (0.887 mm for the x-axis, and 1.100 mm for y-axis; Figure 8 B1).

DISCUSSION

Fracture load is one of the most critical factors in determining the long-term durability of restorations. In this particular study, quasi-static loading of specimens and cyclic aging has been employed to simulate clinical conditions and provide predictions of their long-term success. Based on our results, the fracture resistance of both tested materials either before or after aging exceeded the average occlusal

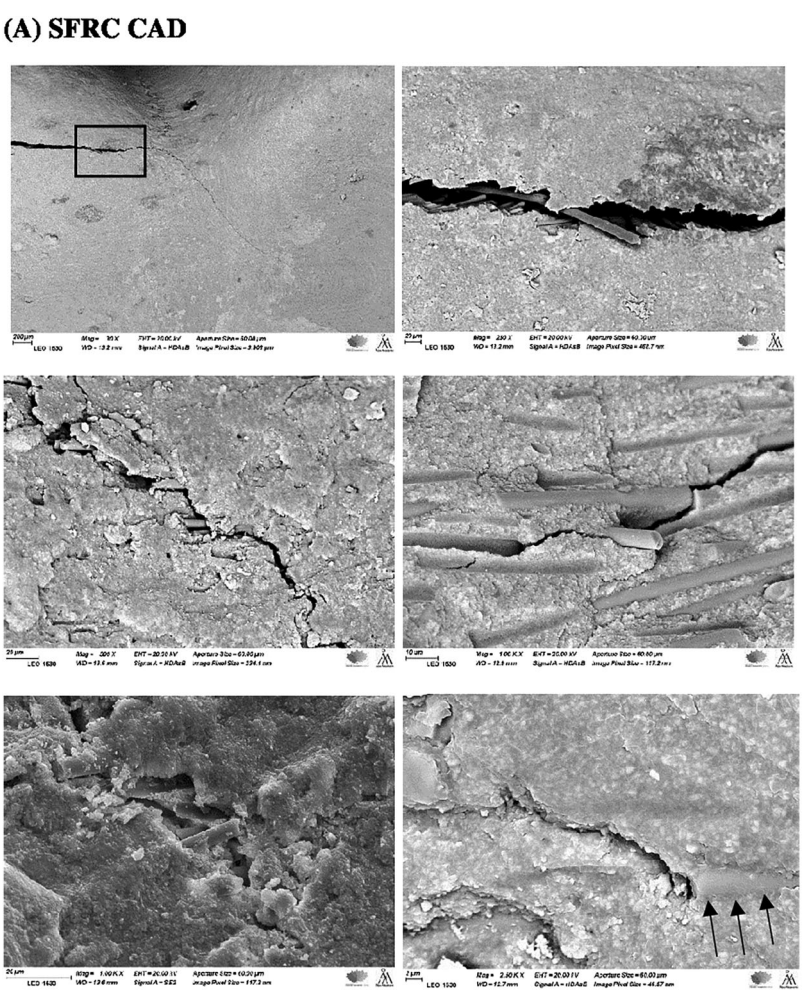

FIGURE 5 Scanning electron microscope images of the specimens after fracture. (A) Short fiber-reinforced composite computer-aided design (SFRC CAD) specimens illustrating the crack pathway. Images display multiple instances of fiber pullout and bridging, leading to the final crack arrest by short fibers (arrows). Magnifications: top left, 30×; top right, 250×; middle left, 500×; middle right, 1000×; bottom left, 1000×; bottom right, 2500×. (B) Lithium-disilicate CAD illustrating typical characteristics of radial brittle fracture pattern with sharp edges. Magnifications: top left, 250×; top right, 500×; bottom left, 1000×; bottom right, 2500×.

European Journal of Oral Sciences NOF Scandinavian Division IADR WILEY

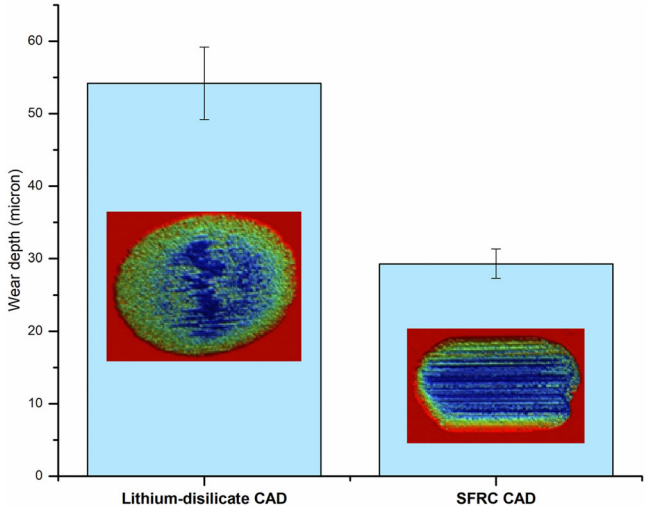

FIGURE 6 The average of maximum wear depth (μm) and standard deviations (bars) of lithium-disilicate computer-aided design (CAD) and short fiber-reinforced composite (SFRC) CAD specimens, and typical 2D surface profiles of the wear trace after wear tests.

force in the posterior region (approximately 800 N) [27]. As mentioned in the results, SFRC CAD FPDs showed higher fracture resistance values before and after cyclic fatigue aging compared to lithium-disilicate FPDs, and the aging process significantly affected the load-bearing capacity of the tested FPDs (Figure 2). Therefore, the hypothesis that material type and aging process have no effect on the fracture resistance of the FPDs cannot be accepted.

One explanation of our results could be due to the typically higher elasticity and toughness of SFRC CAD compared to lithium-disilicate ceramics (Figure 4), which allows the SFRC CAD to absorb and distribute forces more effectively. The experimental SFRC CAD had an average fracture toughness of 2.9 MPa $m^{1/2}$, while the value reported for lithium-disilicate CAD (e.max CAD) in the literature is approximately 1.88 MPa $m^{1/2}$ [26, 28–30]. This property helps in the prevention of crack propagation and reduces the likelihood of catastrophic failure. In contrast, lithium-disilicate ceramics are relatively more brittle and can be prone to cracking or fracturing when subjected to sudden or excessive forces [26, 28]. Our results are in line with previous research which has explained the possible causes behind higher load-bearing capacity of SFRC composite compared to ceramic FPDs. These studies showed that the resiliency of composite FPDs enables them to endure the impact of loading [26, 29]. This is achieved by effectively dispersing destructive fracture energy and undergoing a higher degree of elastic deformation before experiencing failure. From a fractographic perspective, the action of fiber pulling and bridging in SFRC CAD successfully redirected and/or arrested the propagation of cracks (Figure 5A). Thus, the reinforcing mechanism can be attributed to the absorption of fracture crack energy. In contrast, ceramic FPDs, being stiffer in nature, possess a relatively lesser capacity to diffuse fracture energy and undergo elastic deformation, making them more prone to the brittle type of failure under similar loading conditions [26].

Fatigue forms, such as repetitive mechanical loading, significantly impact the fracture resistance of the examined FPDs. However, in our study, the changes significantly varied according to the material used. There was a significant decrease ($p < 0.05$) in the fracture resistance of the SFRC CAD FPDs after cyclic fatigue aging, while the opposite scenario was observed in the lithium-disilicate group, in which there was an increase ($p < 0.05$) after aging in the fracture resistance. This is consistent with the findings of Schultheis et al. [31], who found, when examining the impact of fatigue on the fracture load of monolithic lithium-disilicate CAD posterior three-unit FPDs, that load-bearing capacity increased after aging (1900 N) compared to before aging (1298 N). The possible reason is that repeated cyclic loading in an aqueous environment could induce microstructural changes to the material's properties. These changes may include precipitation or redistribution of reinforcing phases within the lithium-disilicate material, thereby improving its fracture resistance. Moreover, cement plasticization allows for better stress distribution, reducing the likelihood of material failure or fracture under functional loads, and ultimately increasing the overall fracture resistance.

Even when subjected to forces exceeding normal masticatory forces, there were no indications of adhesive failure in any of the FPDs, both before and after aging. This suggests the high effectiveness of bonding. The bonding between the luting resin and CAD/CAM materials is a result of a synergistic combination of chemical bonding, promoted by primer use, and micromechanical retention accomplished through acid etching [25].

Consistent with previous studies, the fracture of our FPD specimens occurs in the connector region due to the concentration of stress in this specific area, regardless of the material used [32, 33]. In FPDs, an even distribution of compressive stress occurs in the occlusal embrasure, while tensile stress is distributed in the gingival embrasure. The stress distribution can be improved by using broadly curved connectors instead of sharply curved ones. As a result, FPDs with sharper connectors have a higher failure rate [34]. According to Oh et al. [35], the fracture resistance of all-ceramic FPDs is significantly influenced by the radius of the connector curvature at the gingival embrasure.

Although the loading cycles were identical in terms of number, frequency, and chewing force, the wear behavior of the tested CAD/CAM blocks varied based on the material type (Figure 6). SFRC CAD showed lower wear depth than lithium-disilicate, and as seen in a previous study [23], microfibers were polished down together with the composite matrix. Lithium-disilicate CAD exhibits wear tracks with

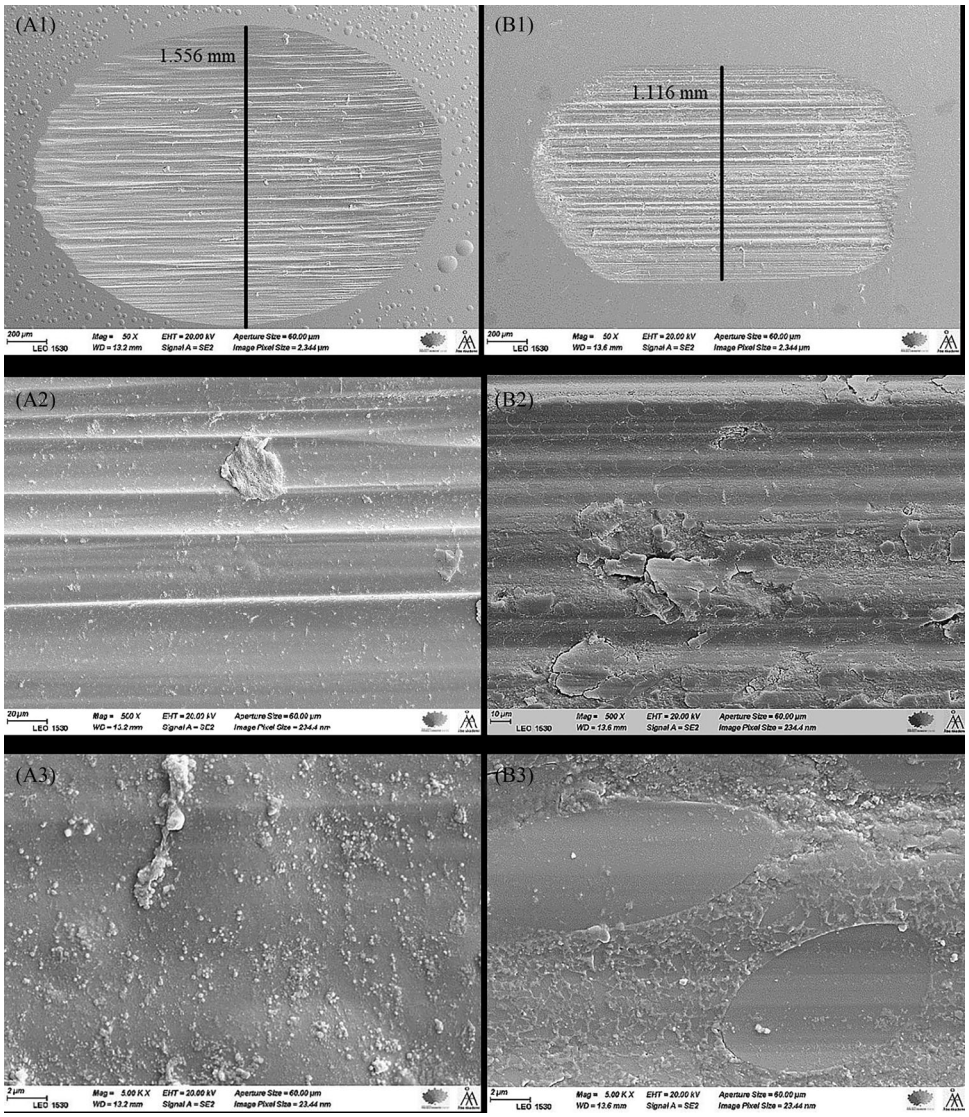

FIGURE 7 Scanning electron microscope images showing wear facets of lithium-disilicate computer-aided design (CAD; A1–3) and short fiber-reinforced composite (SFRC) CAD (B1–3) specimens, with different magnifications (A1, B1: 50×; A2, B2: 500×; A3, B3: 5000×).

smooth, elongated scratches. These scratches are characterized by parallel and fine lines that extend along the length of the wear track. The smooth scratches are seen due to the fineness of the crystalline structures of the lithium-disilicate CAD, which result in fine scratches. Our findings align with a previous study [36], although making a direct comparison could be difficult due to the difference in material-antagonist combinations. In that study [36], resin CAD/CAM materials exhibited satisfactory wear resistance, while lithium-disilicate CAD showed indications of abrasive wear. Conversely, other studies presented entirely contradictory outcomes [37, 38], where composite blocks exhibited greater wear volume loss compared to glass-ceramic materials. Those findings were attributed to the comparatively lower hardness of composites in comparison to the other ceramic CAD/CAM examined in the investigations. However, a previous study indicated that there is a limited correlation between microhardness and abrasive wear, specifically in ceramic materials [39]. The inconsistency in these findings can be linked to variations in wear test conditions and the utilization of different antagonist materials.

Chewing simulators used for wear assessment have employed a range of materials as antagonists, including enamel, ceramics, polymers, and metals. In our research, we utilized a steatite-ceramics ball as the antagonist. This ball is composed of magnesium meta silicate and designed to possess desirable characteristics such as having a non-porous homogenous internal microstructure, being tough, dense, and hard [40]. Vicker's hardness of the steatite ball is 520–550 Hv [40], which is nearly similar to that of IPS e.max (591.4 Hv) [41]. Therefore, due to the positive correlation between the counterface surface hardness and the friction coefficient,

European Journal of Oral Sciences

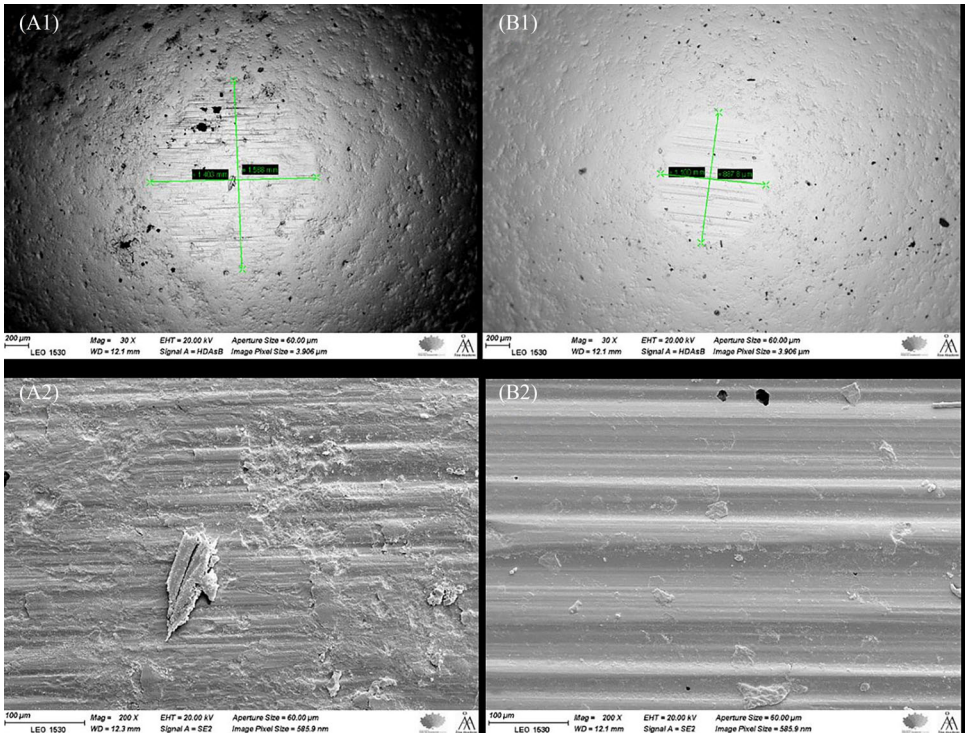

FIGURE 8 Scanning electron microscope images of steatite balls used in wear tests with a chewing simulator. (A1,2) Ball used as antagonist with lithium-disilicate specimens (A1, 30×; A2, 200×). (B1,2) Antagonist ball used with short fiber-reinforced composite computer-aided design (SFRC CAD) specimens (B1, 30×; B2, 200×).

the interaction of two ceramic surfaces with higher hardness can result in significant surface wear. This wear is primarily attributed to the increased hardness, and to frictional and abrasive forces [42, 43]. This is the most plausible explanation for the observed wear results. In line with these findings, when the antagonist wear was also examined, it was noticed that the size of the wear facet of the steatite ball was bigger when lithium-disilicate was used than when SFRC CAD was tested. Notably, the vertical dimensions of wear facets on the specimens and steatite antagonist were highly similar (Figures 7 and 8).

The steatite antagonists exhibited average wear that was found to be lower than the natural wear of tooth enamel [44]. Despite not being regarded as the optimal material in relation to diverse physical properties, incorporating steatite as an antagonist in the in vitro wear tests could yield an unbiased test outcome [45]. Utilizing natural tooth enamel as an antagonist might generate a wear outcome that better emulates clinical conditions; however, the preparation of tooth enamel antagonists poses challenges due to obstacles in attaining uniformity and shaping.

Various factors, such as temperature, masticatory forces, and moisture, can impact the materials' fracture load. Furthermore, it is known that laboratory tests cannot accurately simulate the exact wear conditions experienced by restorative materials clinically [46]. Hence, it is essential to take these variations into account when conducting in vitro studies to extrapolate the findings to clinical settings; moreover, to gain a comprehensive understanding of the material's performance in clinical settings, additional studies are required.

The results of this study have been considered within the context of certain limitations, the number of groups used is one of them since this could affect the generalizability and the variability of the results. Moreover, the used zirconia model could not completely mimic the clinical situation, due to its rigid nature, and elevated elastic modulus surpassing that of dentin. Lastly, the number of cycles applied in the fracture load test (100,000 cycles) doesn't correspond to a long simulated clinical service time.

Considering the limitations of this in vitro study, the findings indicate that the experimental SFRC CAD exhibits the highest load-bearing capacity both before and after cyclic fatigue aging. Moreover, it yielded enhanced wear behavior in comparison to the lithium-disilicate control material.

AUTHOR CONTRIBUTIONS

Conceptualization: Sufyan Garoushi, Pekka Vallittu, Lippo Lassila; Data curation: Sufyan Garoushi; **Formal analysis**: Enas Mangoush, Sufyan Garoushi; **Investigation**: Enas Mangoush; Project administration: Pekka Vallittu, Lippo Lassila; **Software**: Enas Mangoush; **Supervision**: Sufyan Garoushi, Pekka Vallittu, Lippo Lassila; **Validation**: Lippo Lassila;

Writing – original draft: Enas Mangoush; **Writing – review review & editing**: Sufyan Garoushi, Pekka Vallittu, Lippo Lassila.

ACKNOWLEDGMENTS

This study belongs to the research activity of BioCity Turku Biomaterials Research Program (www.biomaterials.utu.fi). In conducting this research, no external funding or financial support was received.

CONFLICT OF INTEREST STATEMENT

One of the authors (V.P.) declares that he is a consultant for Stick Tech oy, a member of GC Company, in the training, research, and development. The other authors confirm that they have no conflicts of interest.

ORCID

Enas Mangoush https://orcid.org/0000-0001-5904-2799
Sufyan Garoushi https://orcid.org/0000-0001-9457-2314
Pekka Vallittu https://orcid.org/0000-0002-9981-6717
Lippo Lassila https://orcid.org/0000-0002-1575-2083

REFERENCES

1. Yoshida T, Kurosaki Y, Mine A, Kimura-Ono A, Mino T, Osaka S, et al. Fifteen-year survival of resin-bonded vs full-coverage fixed dental prostheses. J Prosthodont Res. 2019;63:374–82.
2. Poggio CE, Ercoli C, Rispoli L, Maiorana C, Esposito M. Metal-free materials for fixed prosthodontic restorations. Cochrane Database Syst Rev 2017;12(12):CD009606. http://doi:10.1002/14651858.CD009606.pub2
3. Pjetursson BE, Sailer I, Makarov NA, Zwahlen M, Thoma DS. All-ceramic or metal-ceramic tooth-supported fixed dental prostheses (FDPs)? A systematic review of the survival and complication rates. Part II: Multiple-unit FDPs. Dent Mater. 2015;31:624–39.
4. Sailer I, Makarov NA, Thoma DS, Zwahlen M, Pjetursson BE. All-ceramic or metal-ceramic tooth-supported fixed dental prostheses (FDPs)? A systematic review of the survival and complication rates. Part I: Single crowns (SCs). Dent Mater. 2015;31:603–23.
5. Borba M, de Araújo MD, de Lima E, Yoshimura HN, Cesar PF, Griggs JA, et al. Flexural strength and failure modes of layered ceramic structures. Dent Mater. 2011;27(12):1259–66.
6. Göstemeyer G, Jendras M, Dittmer MP, Bach FW, Stiesch M, Kohorst P. Influence of cooling rate on zirconia/veneer interfacial adhesion. Acta Biomater. 2010;6:4532–8.
7. Guazzato M, Walton TR, Franklin W, Davis G, Bohl C, Klineberg I. Influence of thickness and cooling rate on development of spontaneous cracks in porcelain/zirconia structures. Aust Dent J. 2010;55:306–10.
8. Benli M, Turkyilmaz I, Martinez JL, Schwartz S. Clinical performance of lithium disilicate and zirconia CAD/CAM crowns using digital impressions: a systematic review. Prim Dent J. 2022;11:71–6.
9. Becker M, Chaar MS, Garling A, Kern M. Fifteen-year outcome of posterior all-ceramic inlay-retained fixed dental prostheses. J Dent. 2019. https://doi.org/10.1016/j.jdent.2019.07.012
10. Brandt S, Winter A, Lauer HC, Kollmar F, Portscher-Kim SJ, Romanos GE. IPS e.max for all-ceramic restorations: clinical survival and success rates of full-coverage crowns and fixed partial dentures. Materials (Basel). 2019;12(3):462. https://doi.org/10.3390/ma12030462
11. Tanış MÇ, Akay C, Karakış D. Resin cementation of zirconia ceramics with different bonding agents. Biotechnol Biotechnol Equip. 2015;29:363–7.
12. Özcan M, Bernasconi M. Adhesion to zirconia used for dental restorations: a systematic review and meta-analysis. J Adhes Dent. 2015;17:7–26.
13. Keilig L, Stark H, Bourauel C. Does the material stiffness of novel high-performance polymers for fixed partial dentures influence their biomechanical behavior? Int J Prosthodont. 2016;30:595–7.
14. Lebon N, Tapie L, Vennat E, Mawussi B. Influence of CAD/CAM tool and material on tool wear and roughness of dental prostheses after milling. J Prosthet Dent. 2015;114:236–47.
15. Lassila L, Säilynoja E, Prinssi R, Vallittu PK, Garoushi S. Fracture behavior of Bi-structure fiber-reinforced composite restorations. J Mech Behav Biomed Mater. 2020;101:103444. https://doi.org/10.1016/j.jmbbm.2019.103444
16. Lassila L, Keulemans F, Säilynoja E, Vallittu PK, Garoushi S. Mechanical properties and fracture behavior of flowable fiber-reinforced composite restorations. Dent Mater. 2018;34:598–606.
17. Garoushi S, Mangoush E, Vallittu M, Lassila L. Short fiber reinforced composite: a new alternative for direct onlay restorations. Open Dent J. 2013;7:181–5.
18. Garoushi S, Vallittu PK, Lassila LVJ. Short glass fiber reinforced restorative composite resin with semi-interpenetrating polymer network matrix. Dent Mater. 2007;23:1356–62.
19. Nagata K, Garoushi SK, Vallittu PK, Wakabayashi N, Takahashi H, Lassila LVJ. Fracture behavior of single-structure fiber-reinforced composite restorations. Acta Biomater Odontol Scand. 2016;2:118–24.
20. Garoushi S, Vallittu PK, Lassila LV. Direct restoration of severely damaged incisors using short fiber-reinforced composite resin. J Dent. 2007;35:731–36.
21. Mangoush E, Garoushi S, Vallittu PK, Lassila L. Influence of short fiber- reinforced composites on fracture resistance of single-structure restorations. Eur J Prosthodont Restor Dent. 2020;28:189–98.
22. Jandt KD, Sigusch BW. Future perspectives of resin-based dental materials. Dent Mater. 2009;25:1001–6.
23. Mangoush E, Lassila L, Vallittu PK, Garoushi S. Microstructure and surface characteristics of short- fiber reinforced CAD/CAM composite blocks. Eur J Prosthodont Restor Dent. 2020;28:1–9.
24. Lassila L, Säilynoja E, Prinssi R, Vallittu P, Garoushi S. Characterization of a new fiber-reinforced flowable composite. Odontology. 2019;107:342–52.
25. Mangoush E, Lassila L, Vallittu PK, Garoushi S. Shear-bond strength and optical properties of short fiber-reinforced CAD/CAM composite blocks. Eur J Oral Sci. 2021;129:1–10 https://doi.org/10.1111/eos.12815
26. Lassila L, Mangoush E, Vallittu PK, Garoushi S. Fracture behavior of discontinuous fiber-reinforced composite inlay-retained fixed partial denture before and after fatigue aging. J Prosthodont Res. 2023;67:271–7.
27. Varga S, Spalj S, Lapter Varga M, Anic Milosevic S, Mestrovic S, Slaj M. Maximum voluntary molar bite force in subjects with normal occlusion. Eur J Orthod. 2011;33:427–33.

28. Kassem AS, Atta O, El-Mowafy O. Fatigue resistance and microleakage of CAD/CAM ceramic and composite molar crowns. J Prosthodont. 2012;21:28–32.
29. Awada A, Nathanson D. Mechanical properties of resin-ceramic CAD/CAM restorative materials. J Prosthet Dent. 2015;114:587–93.
30. Belli R, Geinzer E, Muschweck A, Petschelt A, Lohbauer U. Mechanical fatigue degradation of ceramics versus resin composites for dental restorations. Dent Mater. 2014;30:424–32.
31. Schultheis S, Strub JR, Gerds TA, Guess PC. Monolithic and bi-layer CAD/CAM lithium-disilicate versus metal-ceramic fixed dental prostheses: comparison of fracture loads and failure modes after fatigue. Clin Oral Investig. 2013;17:1407–13.
32. Kolbeck C, Rosentritt M, Behr M, Lang R, Handel G. In vitro examination of the fracture strength of 3 different fiber-reinforced composite and 1 all-ceramic posterior inlay fixed partial denture systems. J Prosthodont. 2002;11:248–53.
33. Fischer H, Weber M, Eck M, Erdrich A, Marx R. Finite element and experimental analyses of polymer-based dental bridges reinforced by ceramic bars. J Biomech. 2004;37:289–94.
34. Oh WS, Anusavice KJ. Effect of connector design on the fracture resistance of all-ceramic fixed partial dentures. J Prosthet Dent. 2002;87:536–42.
35. Oh W, Götzen N, Anusavice KJ. Influence of connector design on fracture probability of ceramic fixed-partial dentures. J Dent Res. 2002;81:623–7.
36. Lawson NC, Bansal R, Burgess JO. Wear, strength, modulus and hardness of CAD/CAM restorative materials. Dent Mater. 2016;32:275–83.
37. Zhi L, Bortolotto T, Krejci I. Comparative in vitro wear resistance of CAD/CAM composite resin and ceramic materials. J Prosthet Dent. 2016;115:199–202.
38. An SJ, Lee H, Ahn JS, Lee JH, Lee HH, Choi YS. Influence of thermo-mechanical aging on fracture resistance and wear of digitally standardized chairside computer-aided-designed/computer-assisted-manufactured restorations. J Dent. 2023;130:104450. https://doi.org/10.1016/j.jdent.2023.104450
39. Seghi RR, Rosenstiel SF, Bauer P. Abrasion of human enamel by different dental ceramics in vitro. J Dent Res. 1991;70:221–5.
40. Jyoti Ceramic: steatite ceramic grinding balls Manufacturer & Supplier. Accessed 3 Jul 2023. https://www.jyoticeramic.com/steatite.php
41. Leung BT, Tsoi JK, Matinlinna JP, Pow EH. Comparison of mechanical properties of three machinable ceramics with an experimental fluorophlogopite glass ceramic. J Prosthet Dent. 2015;114:440–6.
42. Oh WS, Delong R, Anusavice KJ. Factors affecting enamel and ceramic wear: a literature review. J Prosthet Dent. 2002;87:451–9.
43. Grigoriev ON, Mazur PV, Neshpor I, Mosina TV, Bega MD, Varchenko V, et al. Wear-resistant TiCN-based ceramic materials for high-load friction units. Powder Metall Met. 2021;59:528–36.
44. León Velastegui M, Montiel-Company JM, Agustín-Panadero R, Fons-Badal C, Solá-Ruíz MF. Enamel wear of antagonist tooth caused by dental ceramics: systematic review and meta-analysis. J Clin Med. 2022;11(21):6547. https://doi.org/10.3390/jcm11216547
45. Shortall AC, Hu XQ, Marquis PM. Potential counter sample materials for in vitro simulation wear testing. Dent Mater. 2002;18:246–54.
46. Heintze SD, Reichl FX, Hickel R. Wear of dental materials: clinical significance and laboratory wear simulation methods -A review. Dent Mater J. 2019;38:343–53.

How to cite this article: Mangoush E, Garoushi S, Vallittu P, Lassila L. Load-bearing capacity and wear characteristics of short fiber-reinforced composite and glass ceramic fixed partial dentures. Eur J Oral Sci. 2023;e12951. https://doi.org/10.1111/eos.12951